2021 43rd Annual International Conference of the
IEEE Engineering in Medicine & Biology Society (EMBC)
Oct 31 - Nov 4, 2021. Virtual Conference

Whole-brain white matter network reorganization in HIV

F. Di Ciò*[1], S.Minosse[1], E. Picchi[1,2], F. Di Giuliano[3], L. Sarmati[4], E. Teti[4], M. Andreoni[4], R. Floris[2], M. Guerrisi[1], F. Garaci[3,5], N. Toschi*[1,6], Senior *Member, IEEE*

***Abstract*— The human immunodeficiency virus (HIV) causes an infectious disease with a high viral tropism toward CD4 T-lymphocytes and macrophage. Since the advent of combined antiretroviral therapy (CART), the number of opportunistic infectious disease has diminished, turning HIV into a chronic condition. Nevertheless, HIV-infected patients suffer from several life-long symptoms, including the HIV-associated neurocognitive disorder (HAND), whose biological substrates remain unclear. HAND includes a range of cognitive impairments which have a huge impact on daily patient life. The aim of this study was to examine putative structural brain network changes in HIV-infected patient to test whether diffusion-imaging-related biomarkers could be used to discover and characterize subtle neurological alterations in HIV infection. To this end, we employed multi-shell, multi-tissue constrained spherical deconvolution in conjunction with probabilistic tractography and graph-theoretical analyses. We found several statistically significant effects in both local (right postcentral gyrus, right precuneus, right inferior parietal lobule, right transverse temporal gyrus, right inferior temporal gyrus, right putamen and right pallidum) and global graph-theoretical measures (global clustering coefficient, global efficiency and transitivity). Our study highlights a global and local reorganization of the structural connectome which support the possible application of graph theory to detect subtle alteration of brain regions in HIV patients.**

***Clinical Relevance*—Brain measures able to detect subtle alteration in HIV patients could also be used in e.g. evaluating therapeutic responses, hence empowering clinical trials.**

I. Introduction

The human immunodeficiency virus (HIV) is an infectious disease with a high viral tropism toward CD4 T-lymphocytes and macrophage. The subsequent immunodepression due to the development of the pathology bring a pronounced reduction of the CD4 T-lymphocytes. The new combined antiretroviral therapy (CART) has greatly reduced the incidence of opportunistic infections, transforming the HIV into a chronic condition. The incidence of HIV-associated neurocognitive disorder (HAND) is still an important problem in the everyday life of HIV patients [1], [2]. While the usage of neurological test can help in assess the neurocognitive impairment, they lack of the sensitivity to identify subtle neurological involvement [3]. Several papers showed alteration in white matter in subjects affected by HIV [4], [5] and in the so called structural connectome [6].

Structural connectivity is described as the presence of physical connection among brain regions constituted by white matter tracts [7], and has been shown to change in the presence of a number of conditions [8] [9]. It is commonly estimated using diffusion weighted imaging (DWI), which allows the indirect reconstruction of the brain white matter (WM) fibers based on estimating the probabilistic displacement profile of water molecules in tissue. To date, the bulk of research on WM composition is performed using diffusion tensor imaging (DTI) [10] in conjunction with deterministic or probabilistic tractography [11]. However the underlying assumption of a one-to-one mapping between the diffusion profile and each voxel and fiber direction cannot adequately resolve the structural complexity of WM microarchitecture at the voxel scale. This limitation can be overcome using more complex acquisition schemes in conjunctions with more advanced methods to model the diffusion signal. In this context, spherical deconvolution [12], and in particular the recently introduced multi-shell, multi-tissue constrained spherical deconvolution [13] technique allows a more accurate estimation of the fiber orientation distribution function (fODF) through the usage of intrinsically generated maps for WM, gray matter (GM) and cerebrospinal fluid (CSF). Also, brain network are often represented as graphs (build using brain regions as nodes and functional or structural connections as edges) and subsequently analyzed using graph-theoretical tools [14], [15]. It has been shown that metrics which summarize e.g. graph topology, efficiency, clustering etc. can convey important information about brain network reorganization [15], [16].

The aim of this study was to examine putative structural brain network changes in HIV-infected patient to test whether diffusion-imaging-related biomarkers could be used to discover and characterize subtle neurological alterations in HIV infection.

MATERIALS AND METHODS

A. Subjects

Fifteen subjects (male 9) HIV infected patients and fifteen age matched healthy controls (male 7) were enrolled at the Department of Infectious Disease of the University Hospital of Rome "Tor Vergata". The study was approved by the local institutional ethics committee and adhered to the tenets of the Declaration of Helsinki. Written informed consent was obtained from all participants. The study protocol was approved by the local Institutional Review Board. Patients were considered eligible in absence of previously diagnosed neurological disorders and were excluded if they had a history of stroke, demyelinating disease, abuse of drugs in the last five years, epilepsy, head trauma, tumors, coinfections and infections of the central nervous system. Patients were undergoing combination antiretroviral therapy (cART). Subjects information are summarized in the Table 1.

B. MRI Acquisition

Magnetic Resonance Imaging (MRI) was performed on a 3-Tesla scanner (Achieva 3T Intera, Philips Healthcare, The Netherlands) equipped with gradients of maximum amplitude

*Correspondig authors : francesco.cio'.20@ucl.ac.uk, toschi@med.uniroma2.it
[1]Department of Biomedicine and Prevention, University of Rome "Tor Vergata", Rome, Italy. [2]Diagnostic Imaging Unit, Department of Biomedicine and Prevention, University of Rome Tor Vergata, Rome, Italy.
[3]Neuroradiology Unit, Department of Biomedicine and Prevention, University of Rome "Tor Vergata", Rome, Italy. [4]Clinical Infectious Diseases, Tor Vergata University, Rome, Italy. [5]San Raffaele Cassino, Frosinone, Italy. [6]Athinoula A. Martinos Center for Biomedical Imaging, Harvard Medical School, Boston, MA, United States.

of 80 mT/m and rise time of 200 mT/m/ms and a dedicated 8-channel head coil. The MR protocol included a T1-weighted high-resolution sequence obtained using a three dimensional magnetization prepared rapid gradient echo (MPRAGE) with the following parameters: FOV: 256x240 mm^2, voxel size 1x1x1.2 mm^3, TR 500 ms, TE 50 ms and flip angle 8°. Diffusion weighted image was acquired using a Spin-Echo Echo Planar single-shot sequence with the sequent parameters: TR 7,774 ms, TE 89 ms, FOV 240x240, voxel size 2.5 mm (isotropic), SENSE reduction factor R=2. We acquired eight non diffusion weighted image and two distinct b-values, respectively 1000 s/mm² and 2500 s/mm² in 32 noncoplanar and noncollinear directions. Moreover, for each subject, a T1 weighted sagittal TSE, a T2 weighted axial TSE, an axial T2 fluid attenuated inversion recovery and a 3D-T1 FFE were collected and an expert neuroradiologist used them to exclude visible abnormalities.

TABLE I. CLINICAL CHARACTERISTIC OF THE POPULATION STUDY

	HIV	HC
Group size	15	15
Age (years) Average (range)	41 (26-65)	45(27-64)
Sex (Male/Female)	(9/5)	(7/8)
Ethnicity		
Caucasian	13	15
Hispanic	2	--
Risk factor, n		
Heterosexual	8	20
Homosexual	6	--
Intravenous Drug Users	1	--
Duration cART at MRI days		
median [min, max]	106.5 [0-5717]	--

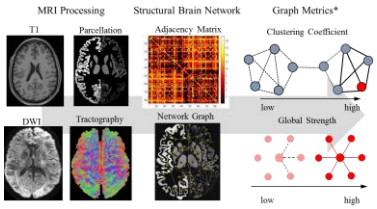

Figure 1. Analysis Workflow.

C. MRI Analysis

The overall analysis workflow is depicted in Figure 1. The preprocessing of the T1 weighted image carried out as follows: we used BET (FSL tool) [17], [18] to remove the skull surface and FAST [19] to segment the brain in three tissue type GM, WM and CSF. Finally, we used the FreeSurfer [20] reconstruction stream to obtain a subject-wise cortical parcellation based on the Desikan-Killany atlas. The subcortical parcels obtained using the volume estimation from FAST [21] were included in the final parcellation. DWI data was processed as follows. First, noise level was estimated and denoising was applied using tools from random matrix theory [22]–[24] in the software package MRtrix [25]. Subsequentially, we corrected for geometric distortion, subject motion and eddy-current induced distortion through EDDY tool [19], also part of FSL [18]. We then registered [26] the T1-weighted image to the DWI image for each subject using ANTs (http://stnava.github.io/ANTs/). We then obtained the WM fODF by first computing the response function (RF) [13] and then using multi-shell, multi-tissue CSD. Finally, based on the fODF estimations, we created a whole brain tractogram using probabilistic tractography [21], [27], [28]. For each subject, we traced 100 million streamlines and successively filtered them down to 10 million by using Spherical-deconvolution Informed Filtering Tractograms (SIFT) [29].

C. Graph theoretical analysis

By superimposing the subject-wise parcellation onto the tractograms, we obtained a connectome, i.e. a comprehensive map of estimated WM tracts across the whole brain. The resulting brain network was used to compute graph theory metrics for each subject. We calculated both local and global metrics: betweenness centrality and local strength (centrality measures) and local efficiency and local clustering coefficient (functional segregation metrics). The global metrics we employed were as follows: global efficiency, global clustering coefficient, global strength and transitivity [16] (Figure 2). All the aforementioned measures were calculated using the Brain Connectivity Toolbox [15].

All graph theoretical measures were compared between HIV groups and HC groups using the non-parametric Mann Whitney U Test, whose results were corrected for multiple comparisons across all 84 regions included in the parcellation using a false rate discovery rate (FDR) procedure (alpha = 0.05). A p-value < 0.05 was considered statistically significant. Also, for each comparison, we estimated effect size as a percentage of median group-wise difference ($\Delta(M_H - M_C)$, M_H: HIV's median in the HIV group, M_C: Median in the HC group).

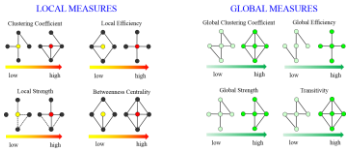

Figure 2 Illustration of global (right) and local (left) graph theoretical metrics

II. RESULTS

We found statistically significant differences between the HIV-infected group and the control group in both local and global metrics. We found statistically significant differences in both global clustering coefficient (p=.013, HC>HIV), global efficiency (p=.036, HC>HIV) and transitivity (p=.009, HC>HIV). No statistically significant difference was observed in global strength. (Figure 3).

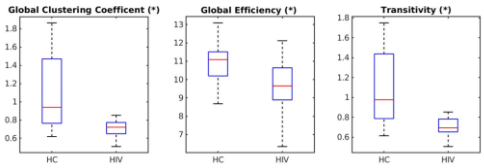

Figure 3 : Global metrics in which group-wise, statistically significant differences were found. HC= healthy controls. (*) p<0.05

Additionally, concerning local metrics, we found statistically significant differences in betweenness centrality in the right inferior temporal gyrus (p=.015, HIV>HC), in the right transverse temporal gyrus (Herschel gyrus) (p=.005, HC>HIV) (Figure 4, Table 2) and in the right pallidum (p=.04, HC>HIV). Differences were also observed in local strength (Figure 5, Table 2). Additionally, we found statistically significant differences in both local clustering coefficient and local efficiency in the right pallidum (clustering coefficient

p= .01 HC>HIV, local efficiency p= .007 HIV>HC), in the right putamen (clustering coefficient p= .005 HC>HIV, local efficiency p= .007 HIV>HC), in the right inferior parietal lobule (clustering coefficient p= .004 HC>HIV, local efficiency p= .007 HIV>HC), in the postcentral gyrus (clustering coefficient p= .004 HC>HIV, local efficiency p= .003 HC>HIV) and in the precuneus (clustering coefficient p= .007 HC>HIV, local efficiency p= .01 HIV>HC) (Table 2, Figure 4).

TABLE II.

Region	Graph theory measures	**p-value**	Δ (M_H - M_C)
R - postcentral gyrus	Clustering Coefficient	0.004	-74%
	Local Efficiency	0.003	-15%
R - precuneus	Clustering Coefficient	0.007	-60%
	Local Efficiency	0.01	6%
R – inferior parietal lobule	Clustering Coefficient	0.004	-79%
	Local Efficiency	0.007	22%
R - transverse temporal gyrus	Local Strength	0.005	-14%
R - inferior temporal gyrus	Betweenness Centrality	0.015	55%
R - putamen	Clustering Coefficient	0.005	-33%
	Local Efficiency	0.007	13%
R - pallidum	Clustering Coefficient	0.01	-56%
	Local Efficiency	0.007	12%
	Local Strength	0.04	-2%

Left to right: cerebral region, local measure, p-value ((*) p<0.05) M_H: HIV's median, M_C: Healthy Control's median.

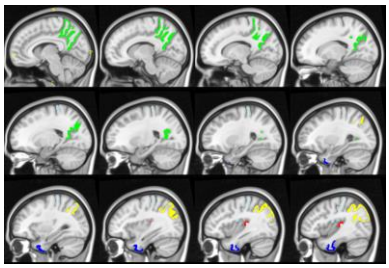

Figure 4 Brain regions that present statistically significant differences in local metrics (S=superior, I=inferior, A=anterior and P=posterior). Legend: precuneus (green), transverse temporal gyrus (red), inferior parietal lobule (yellow), inferior temporal gyrus (blue) and post-central gyrus (light blue). See table II for effect sizes and directions.

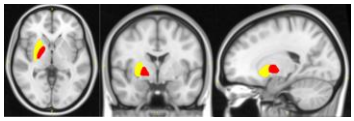

Figure 5 Brain regions that present statistically significant differences in local metrics (L=left, R=right, A=anterior and P=posterior). Legend: Putamen (yellow) and Globus Pallidus (red).

III. Discussion and Conclusion

In this study, we employed multi-shell, multi tissue probabilistic tractography based on spherical deconvolution in conjunction with graph-theory to evaluate putative structural connectivity changes in HIV subjects. We found several statistically significant differences in global metrics: global clustering coefficient, global efficiency and transitivity, highlighting a global reorganization of the structural connectome.

The principal clinical manifestations of the HAND syndrome are attentional deficits, memory and executive function impairment. With the progress of the disease, patients usually are affected by depression and other affective symptoms with signs of psychomotor slowing [1]. Related to this symptomatology, we found several statistically significant differences in brain regions that have a role in these functions. For instance, we found lower clustering coefficient and higher local efficiency in the precuneus in HIV-infected patients as compared to controls. The precuneus is involved in several functions [30]: from visuo-spatial imagery, episodic memory and self-processing operations. It is also involved in executive functions [31]. This region is part of the default mode network [32] and functional modifications of the latter has been highlighted in HIV patients [33]. Moreover, we found lower clustering coefficient and higher local efficiency in the right inferior parietal lobule in HIV-infected patients as compared to controls. This region is involved in several higher cognitive function [34]. In particular, it is part of the cingulo-opercular and ventral attention network, involved in cognitive control and executive function. Furthermore, we found lower betweenness centrality in the inferior temporal gyrus. This region is intercalated in the visual ventral stream, and is involved in higher visual processing as well as in memory processes [35]. Additionally, we found modification of local efficiency and clustering coefficients in the right putamen and also in the local strength in the right pallidum. Together, these two nuclei form the dorsal part of the striatum, which is involved in motor functions, executive functions and stimulus response learning, in line with the motor difficulties experienced by HIV-patients affected by HAND [1], [36].

We also found lower local strength in HIV-infected patients compared to controls in the transverse temporal gyrus. This region is fundamental for auditory processing, and a recent study has highlighted [37] that HIV patients have a central auditory processing deficit.

Taken together, the structural connectivity modification in HIV-infected patients could highlight possible local adaptation of the brain networks as a result of infection. The reduction, and in some case increase (with a possible compensatory role), of the local clustering coefficient and local efficiency highlights dysfunctions in the underlying ability of these region to carry out specialized functional processes, which could be reflected in the symptomatology observed in HIV-infected patients affected by HAND. Similar considerations hold for our observations in betweenness centrality and local strength. These are measures of centrality, i.e. they assess the importance of a specific node in a brain network. These nodes have an essential role in bridging

different regions and sub-regions of the brain, which in turns is fundamental for the correct execution of higher cognitive function in the brain. This could be speculated as a clue to the inclusion of HAND affected HIV-patients in the broad and heterogeneous groups of so-called "disconnection syndromes".

In conclusion, our study highlights a global and local reorganization of the structural connectome in HIV patients compared to HC, with involvement in several regions that subserve functions which are known to be impaired in HAND. Our findings therefore point toward the possibility of examining and monitoring disease presence and progression, and in particular brain involvement, in HIV-infected patients. Although all the statistically significant differences among brain regions are located in the right hemisphere, we did not formally test for possible lateralization effects. To confirm these hypotheses, our findings should be further studied and corroborated in longitudinal study and with larger sample size.

REFERENCES

[1] C. Eggers *et al.*, "HIV-1-associated neurocognitive disorder: epidemiology, pathogenesis, diagnosis, and treatment," *Journal of Neurology*, vol. 264, no. 8. Dr. Dietrich Steinkopff Verlag GmbH and Co. KG, pp. 1715–1727, 01-Aug-2017.

[2] R. K. Heaton *et al.*, "Neurocognitive change in the era of HIV combination antiretroviral therapy: The longitudinal CHARTER study," *Clin. Infect. Dis.*, vol. 60, no. 3, pp. 473–480, Feb. 2015.

[3] E. T. Overton *et al.*, "Performances on the cogstate and standard neuropsychological batteries among HIV patients without dementia," *AIDS Behav.*, vol. 15, no. 8, pp. 1902–1909, Nov. 2011.

[4] O. Davies *et al.*, "Clinical and neuroimaging correlates of cognition in HIV," *J. Neurovirol.*, vol. 25, no. 6, pp. 754–764, 2019.

[5] A. M. Behrman-Lay, R. H. Paul, J. Heaps-Woodruff, L. M. Baker, C. Usher, and B. M. Ances, "Human immunodeficiency virus has similar effects on brain volumetrics and cognition in males and females," *J. Neurovirol.*, vol. 22, no. 1, pp. 93–103, 2016.

[6] R. P. Bell, L. L. Barnes, S. L. Towe, N. kuei Chen, A. W. Song, and C. S. Meade, "Structural connectome differences in HIV infection: brain network segregation associated with nadir CD4 cell count," *J. Neurovirol.*, vol. 24, no. 4, pp. 454–463, 2018.

[7] L. Q. Uddin, "Complex relationships between structural and functional brain connectivity," *Trends Cogn. Sci.*, vol. 17, pp. 600–602, 2013.

[8] M. Pievani, N. Filippini, M. P. Van Den Heuvel, S. F. Cappa, and G. B. Frisoni, "Brain connectivity in neurodegenerative diseases - From phenotype to proteinopathy," *Nat. Rev. Neurol.*, 2014.

[9] F. Di Ciò *et al.*, "Reorganization of the structural connectome in primary open angle Glaucoma," *NeuroImage Clin.*, 2020.

[10] P. J. Basser, J. Mattiello, and D. Lebihan, "Estimation of the Effective Self-Diffusion Tensor from the NMR Spin Echo," *J. Magn. Reson. Ser. B*, 1994.

[11] P. Mukherjee, J. I. Berman, S. W. Chung, C. P. Hess, and R. G. Henry, "Diffusion tensor MR imaging and fiber tractography: Theoretic underpinnings," *American Journal of Neuroradiology*, vol. 29, no. 4. American Journal of Neuroradiology, pp. 632–641, 01-Apr-2008.

[12] J. D. Tournier, F. Calamante, D. G. Gadian, and A. Connelly, "Direct estimation of the fiber orientation density function from diffusion-weighted MRI data using spherical deconvolution," *Neuroimage*, 2004.

[13] B. Jeurissen, J. D. Tournier, T. Dhollander, A. Connelly, and J. Sijbers, "Multi-tissue constrained spherical deconvolution for improved analysis of multi-shell diffusion MRI data," *Neuroimage*, vol. 103, pp. 411–426, 2014.

[14] A. Fornito, A. Zalesky, and E. T. Bullmore, *Fundamentals of Brain Network Analysis*. 2016.

[15] M. Rubinov and O. Sporns, "Complex network measures of brain connectivity: Uses and interpretations," *Neuroimage*, 2010.

[16] A. Conti, A. Duggento, M. Guerrisi, L. Passamonti, I. Indovina, and N. Toschi, "Variability and reproducibility of directed and undirected functional MRI connectomes in the human brain," *Entropy*, vol. 21, no. 7, pp. 1–12, 2019.

[17] S. M. Smith, "Fast robust automated brain extraction," *Hum. Brain Mapp.*, 2002.

[18] M. Jenkinson, C. F. Beckmann, T. E. J. Behrens, M. W. Woolrich, and S. M. Smith, "Review FSL," *Neuroimage*, 2012.

[19] S. M. Smith *et al.*, "Advances in functional and structural MR image analysis and implementation as FSL," in *NeuroImage*, 2004.

[20] B. Fischl, "FreeSurfer," *NeuroImage*. 2012.

[21] R. E. Smith, J. D. Tournier, F. Calamante, and A. Connelly, "Anatomically-constrained tractography: Improved diffusion MRI streamlines tractography through effective use of anatomical information," *Neuroimage*, vol. 62, no. 3, pp. 1924–1938, 2012.

[22] J. Veraart, E. Fieremans, and D. S. Novikov, "Diffusion MRI noise mapping using random matrix theory," *Magn. Reson. Med.*, 2016.

[23] J. Veraart, D. S. Novikov, D. Christiaens, B. Ades-aron, J. Sijbers, and E. Fieremans, "Denoising of diffusion MRI using random matrix theory," *Neuroimage*, 2016.

[24] L. Cordero-Grande, D. Christiaens, J. Hutter, A. N. Price, and J. V. Hajnal, "Complex diffusion-weighted image estimation via matrix recovery under general noise models," *Neuroimage*, 2019.

[25] J. D. Tournier *et al.*, "MRtrix3: A fast, flexible and open software framework for medical image processing and visualisation," *NeuroImage*. 2019.

[26] R. Guidotti *et al.*, "Optimized 3D co-registration of ultra-low-field and high-field magnetic resonance images," *PLoS One*, vol. 13, no. 3, p. e0193890, Mar. 2018.

[27] F. C. and A. C. J-D. Tournier, "Improved probabilistic streamlines tractography by 2 nd order integration over fibre orientation distributions," *Ismrm*, vol. 88, no. 2003, p. 2010, 2010.

[28] R. E. Smith, J. D. Tournier, F. Calamante, and A. Connelly, "The effects of SIFT on the reproducibility and biological accuracy of the structural connectome," *Neuroimage*, 2015.

[29] R. E. Smith, J. D. Tournier, F. Calamante, and A. Connelly, "SIFT: Spherical-deconvolution informed filtering of tractograms," *Neuroimage*, 2013.

[30] A. E. Cavanna and M. R. Trimble, "The precuneus: a review of its functional anatomy and behavioural correlates," *Brain*, vol. 129, no. 3, pp. 564–583, Mar. 2006.

[31] B. M. Bettcher *et al.*, "Neuroanatomical substrates of executive functions: Beyond prefrontal structures," *Neuropsychologia*, vol. 85, pp. 100–109, May 2016.

[32] M. E. Raichle, "The Brain's Default Mode Network," *Annu. Rev. Neurosci.*, vol. 38, pp. 433–447, Jul. 2015.

[33] J. B. Thomas, M. R. Brier, M. Ortega, T. L. Benzinger, and B. M. Ances, "Weighted brain networks in disease: Centrality and entropy in human immunodeficiency virus and aging," *Neurobiol. Aging*, vol. 36, no. 1, pp. 401–412, Jan. 2015.

[34] K. M. Igelström and M. S. A. Graziano, "The inferior parietal lobule and temporoparietal junction: A network perspective," *Neuropsychologia*, vol. 105, pp. 70–83, Oct. 2017.

[35] Y. Miyashita, "Inferior Temporal Cortex: Where Visual Perception Meets Memory," *Annu. Rev. Neurosci.*, vol. 16, no. 1, pp. 245–263, Mar. 1993.

[36] S. Minosse *et al.*, "Functional brain network reorganization in HIV infection," *J. Neuroimaging*, p. jon.12861, Apr. 2021.

[37] Y. Zhan, J. C. Buckey, A. M. Fellows, and Y. Shi, "Magnetic Resonance Imaging Evidence for Human Immunodeficiency Virus Effects on Central Auditory Processing: A Review," *J. AIDS Clin. Res.*, vol. 08, no. 07, 2017.